Ultra Broadband Ferrite Transmission Line Transformer

Johannes Horn and Georg Boeck

Berlin University of Technology, Microwave Engineering Group

Abstract — **A ferrite transmission line transformer with an impedance transformation of 1:4 and a bandwidth of 1 MHz to 5 GHz is presented. The circuit is based on a straight semi-rigid coaxial transmission line and a single ferrite tube mounted on a PCB. Analysis and modeling of the circuit is presented together with theoretical and experimental results.**

I. Introduction

Transmission line transformers (TLTs) provide bandwidths and power handling capabilities which strongly exceed that one of conventional transformers. The impedance transformation ratio is however restricted to discrete values $1{:}n^2$, where n is the number of parallel lines.

Transmission line transformers are widely used in wideband power amplifiers and balanced mixers and have been described by various authors, [1]-[3]. Typical structures consist of bifilar or coaxial transmission lines wound on ferrite rings, with bandwidths up to some hundred MHz and power handling capabilities reaching into the kW range. The ferrites used for these applications are usually small compared to wavelengths. These TLTs are modeled with good accuracy using lumped element equivalent circuits to represent the electromagnetic field within the ferrite while employing transmission lines for the signal path [2]-[3].

TLTs are used also for the generation of high-power high-voltage pulses. Tens of kVs at nanoseconds risetime can be obtained using structures in the meter range with several paralleled coaxial lines and high impedance ratios. Wound as well as straight structures are used, both with or without ferrite. Also these large transformers have been described with lumped element circuitry [4].

II. New Concept; Functionality

The TLTs presented here are designed for wideband medium-power amplifier matching purposes. The main objective is the extension of the operating bandwidth to much higher frequencies as realizable by conventional transformers. Therefore, a straight TLT layout is chosen to omit parasitic coiling capacitances.

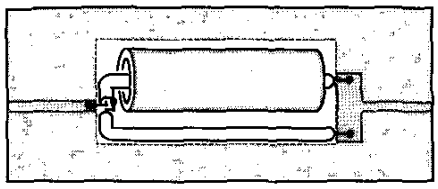

Fig. 1. Transformer arrangement. Two coaxial lines and a ferrite tube are mounted into a rectangular aperture, cutted out from the PCB.

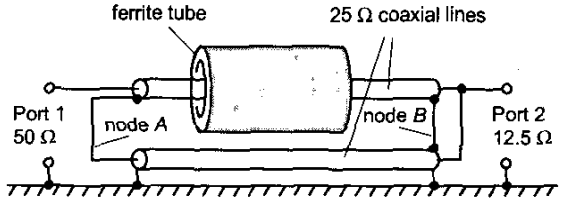

Fig. 2. Schematic circuit diagram of the TLT.

Fig.1 shows the transformer arrangement. Two semi-rigid coaxial lines are mounted into a rectangular aperture cutted out from the PCB. One of the coaxial lines is lead through a ferrite tube. On the lefthand side they are connected to a microstrip line that constitues the 50 Ω port. To the right they are connected to two vertical microstrip lines that meet to constitute the 12.5 Ω port. The aperture opening is 9 mm by 12 mm. The coaxial lines have a characteristic impedance of 25 Ω

From the simplified circuit given in Fig. 2 we can take the functional principle of the impedance transformation. A serial splitter divides the incoming power at the 50 Ω port on the two 25 Ω lines. After passing through these two lines, that must be equal in length, the two signals are combined in parallel to 12.5 Ω. The transformation only works as long as the currents outside of the outer coaxial conductors are negligible. Hence the absolute value of the parasitic shunt impedance at node *A* must be large compared to 25 Ω over the whole frequency range. This requirement can be fulfilled by a large inductance at low frequencies, which is provided by the ferrite. At higher frequencies the short circuit at node *B* is transformed to node *A* along the parasitic transmission line, that is formed by the outer coaxial conductors, the ferrite tube and the

0-7803-7695-1/03/$17.00 © 2003 IEEE

ground of the PCB. The characteristic impedance of that line must be as high as possible in order to yield a sufficiently large parasitic shunt impedance at node *A* over a wide frequency range.

At first sight the upper frequency limit of the TLT is given, when the length between deviding point (node *A*) and short (node *B*) equals half a wavelength of the parasitic mode. In this case one would expect a virtual short to appear at node *A*. However, due to the strong magnetic losses of the ferrite material at higher frequencies, this effect is considerably diminished. With proper choice of the ferrite length and thickness, the operating bandwidth of the TLT is limited by parasitic inductances rather than half-wave transformation.

III. Analysis; Modeling

A. Ferrite properties

The quantities needed to describe the ferrite material in a field analysis are the complex relative permeability $\underline{\mu}_r = \mu_r' - j\mu_r''$ with the imaginary part representing the magnetic losses, the relative permittivity ε_r, and the conductivity σ. For NiZn ferrites the latter is negligible over the whole frequency range.

The ferrite bulk properties are not only dependent on the material composition but also on the manufacturing process, where multiple grains are baked together. The poly grain structure contributes to the frequency dependence of the material constants. A consequence is that properties of the same ferrite type can differ for varying core sizes.

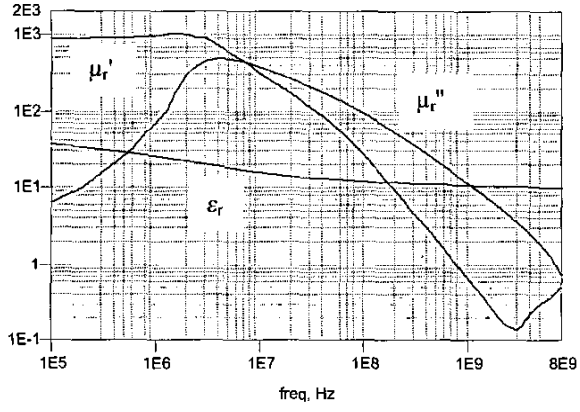

Fig. 3. Real and imaginary part of the complex relative permeability $\underline{\mu}_r = \mu_r' - j\mu_r''$ and relative permittivity ε_r. (FERROXCUBE NiZn ferrite 4S2).

The high frequency permeability data are usually not available from manufacturers. They were measured using precision coaxial lines that were loaded with small ferrite tubes. The results are shown in Fig 3. Above 1 GHz the ferrite behavior is paramagnetic. However, in this frequency range μ_r'' is considerably larger than μ_r' and magnetic losses determine the wave propagation within the ferrite. The gathered μ'-data may therefore be slightly imprecise. At the same time it takes only minor influence on the wave propagation analysis that follows in the next subsection.

It shall be noted that measurements on different NiZn ferrite grades, provided by different manufacturers have shown very similar values of μ' and μ'' in the high-frequency range (100 MHz ... 10 GHz).

The relative permittivity in Fig. 3 was taken from the data sheet of a typical NiZn ferrite.

B. Propagation properties of the parasitic mode

For an investigation of the parasitic mode the structure shown in Fig. 4 is analyzed. In our approach we assume that only one mode propagates in the frequency range of interest and that it can be considered as quasi-TEM. The latter is vital to the whole approach presented here, because it provides that voltage and current, needed in the next subsection to calculate the parasitic line input impedance, are well defined.

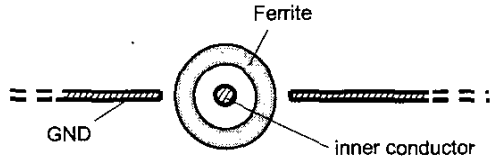

Fig. 4. Cross-section of the analyzed waveguide

While the exact wave propagation constants can be obtained through numerical mode analysis, the quasi-TEM assumption provides insights into their relation to the ferrite properties, especially with dominating magnetic losses. The propagation quantities $\underline{\gamma}$ and $\underline{Z}_L$ are related to the quasi-static inductance $\underline{L}'$ and capacitance C' per unit length by

$$\underline{\gamma} = j\frac{2\pi}{\lambda} + \alpha = \omega \cdot \sqrt{-\underline{L}' \cdot C'} \qquad (1)$$

$$\underline{Z}_L = \sqrt{\frac{\underline{L}'}{C'}} \qquad (2)$$

Due to the magnetic losses, $\underline{L}'$ is complex and consequently $\underline{\gamma}$ and $\underline{Z}_L$ as well. In the frequency range where loss is dominating, the phases of $\underline{\gamma}$ and $\underline{Z}_L$ will be almost +45 DEG and -45 DEG respectively. The wavelength λ and the loss coefficient α are then related by

$$\frac{1}{\alpha} \approx \frac{\lambda}{2\pi} \qquad (3)$$

The propagation properties were calculated using the FDFD method. A comparison to quasi-static calculation results verified the quasi-TEM assumption. The deviation from the accurate value was less than 3 per cent ($|1-\gamma_{TEM}/\gamma| \le 0.03$). The propagation constants and the characteristic impedance are shown in Fig. 5 and Fig. 6.

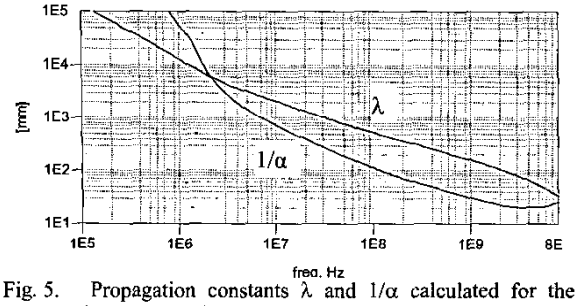

Fig. 5. Propagation constants λ and $1/\alpha$ calculated for the waveguide shown in Fig. 4.

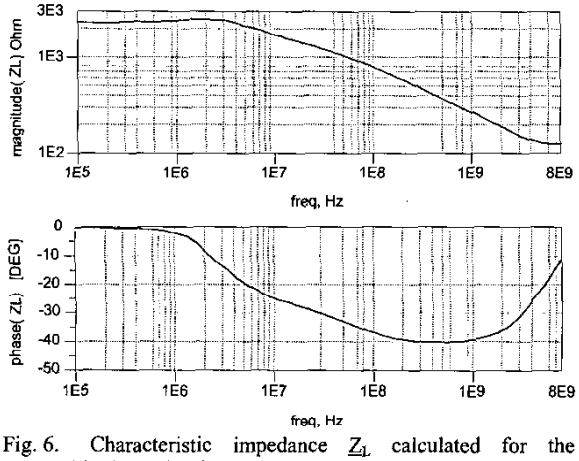

Fig. 6. Characteristic impedance $\underline{Z_L}$ calculated for the waveguide shown in Fig. 4.

C. Parasitic impedance

With the results presented above the parasitic shunt impedance at node *A* of Fig. 2 can be calculated for any length using the equivalent circuit shown in Fig. 7. Two lumped inductors represent the step in width at the feeding point (*A* in Fig. 2) and the non-ideal short circuit at the shorting point (*B* in Fig. 2). An estimate of $L_{step} \approx 0.9$ nH was taken from measurements on lines with various lengths both with and without ferrite.

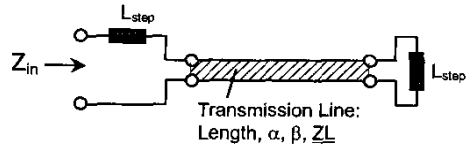

Fig. 7. Equivalent circuit used to calculate the parasitic shunt impedance.

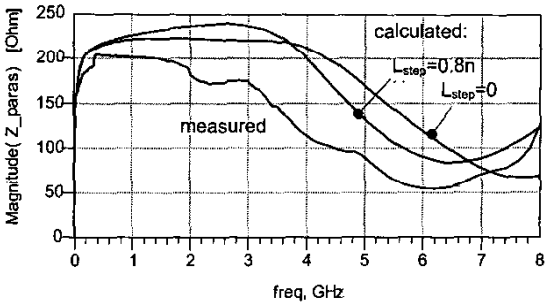

Fig. 8. Parasitic shunt impedance of a 16 mm long structure. Calculations were done with and without L_{step}.

The influence of L_{step} is demonstrated in Fig. 8, where the magnitude of the impedance is depicted for a 16 mm long structure. The minimum at 6 GHz is caused by half-wave impedance transformation. The structure width, represented by L_{step}, appears as a virtual line lengthening that shifts the minimum to lower frequencies.

The parasitic impedance characteristic in the example above would clearly limit the bandwidth of the TLT. A more favourable result can be achieved with a shorter structure. Fig. 9 shows the impedance of a 10 mm long line in a polar plot. Compared to Fig. 8 the minimum occurs at a higher frequency. In addition the maximum value has increased.

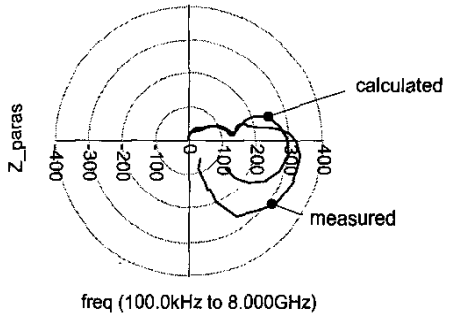

Fig. 9. Parasitic shunt impedance of a 10 mm long structure.

D. Simulated TLT response

The complete equivalent circuit of the TLT is shown in Fig. 10. It mainly consists of three transmission lines, two of them to represent the coaxial lines, and one for the parasitic ferrite loaded line. The length of these lines is equal to the length of the TLT structure. The width is taken into account by additional lines (vertically drawn). The losses of the microstrip lines and the coaxial lines can be neglected in a first order approximation.

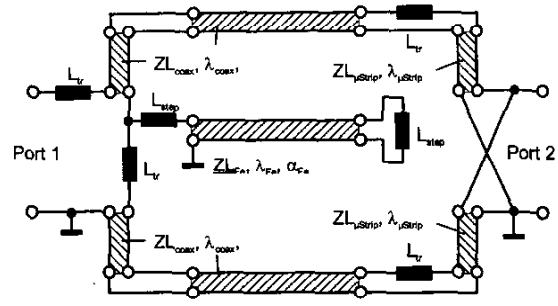

Fig. 10. Equivalent circuit of the TLT

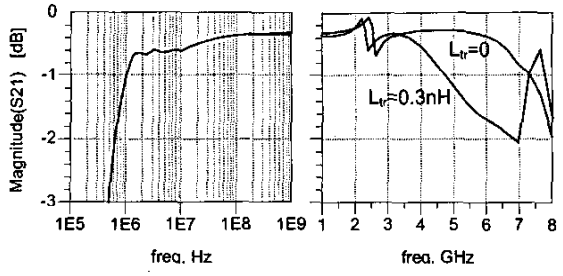

Fig. 11. Expected frequency response S_{21} of the TLT, calculated from the equivalent circuit in Fig. 10 with $L_{tr} = 0$ and $L_{tr} = 0.3$ nH. Port1: 50 Ω; Port2: 12.5 Ω.

In addition to the inductors L_{step} that were discussed in the previous subsection, four more lumped inductors L_{tr} are introduced, representing the coax-microstrip transitions and the series interconnection at the dividing point (*A* in Fig. 2). The impact of L_{tr} on the transformer frequency response is shown in Fig. 11. The expected transmission S_{21} of the structure in Fig. 1 was calculated twice. First the coax-microstrip transitions were neglected ($L_{tr} = 0$) and then $L_{tr} = 0.3$ nH was estimated. The right Fig. shows that the parasitic inductances L_{tr} limit the bandwidth strongly.

IV. Results

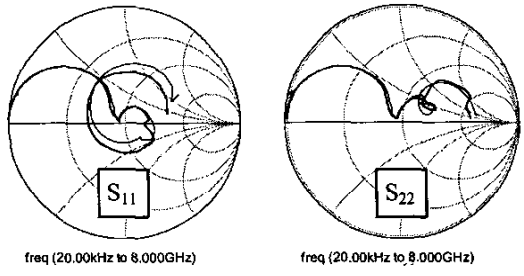

Fig. 12. Frequency response of the TLT input and output reflection coefficients S_{11} and S_{22}, measured (—) and calculated (---). Port1: 50 Ω; Port2: 12.5 Ω.

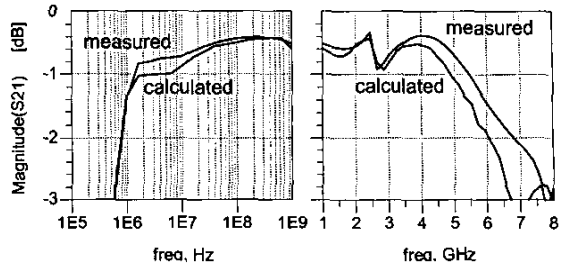

Fig. 13. Frequency response S_{21} of the TLT transmission, measured (—) and calculated (---). Port1: 50 Ω; Port2: 12.5 Ω.

The measured transformer transmission and port reflection are shown in Fig. 12 and Fig. 13 together with simulated results. The four inductances $L_{tr,i}$ and the characteristic impedance $Z_{L,coax}$ of the coaxial lines were optimized in this simulation to fit the measurement. For the inductances $L_{tr,i}$ values between 0.2 nH and 0.7 nH were found and $Z_{L,coax}$ was determined to 29 Ω.

V. Conclusion

An ultra wideband TLT was fabricated based on a single ferrite tube. An analysis of the small signal frequency response was presented, that uses line theory to describe the wave propagation within the ferrite. By taking advantage of quarter-wave impedance transformation along the ferrite line, a high upper frequency limit could be achieved. This was only limited by the parasitic inductance of the coax-microstrip transitions.

Acknowledgement

The authors would like to thank the Microwave Department at Ferdinand-Braun-Institut für Höchstfrequenztechnik, Berlin for allowing and assisting the use of their EM analysis software.

References

[1] C. L. Ruthroff, "Some Broadband Transformers", *Proceedings of the IRE*, vol. 47, pp. 1337-1342, August 1959.

[2] O. Pitzalis Jr. and T. P. Couse, "Practical Design Information for Broadband Transmission Line Transformers", *Proceedings of the IEEE*, vol. 56, no. 4 (Proceedings Letters), pp. 738-739, April 1968.

[3] H. W. Krauss and C. W. Allen, "Designing torrodial transformers to optimize wideband performance", *Electronics*, pp. 113 -116, August 1973

[4] P. W. Smith and J. O. Rossi, "The frequency response of transmission line (cable) transformers", *11th IEEE International Pulsed Power Conference*, Digest of Technical Papers, vol. 1, pp. 610 -615, June 1997